# Biodegradable pH-responsive hydrogels for controlled dual-drug release

Journal of Materials Chemistry B

PAPER



Cite this: J. Mater. Chem. B, 2018, 6, 510

# Biodegradable pH-responsive hydrogels for controlled dual-drug release†

Liang Xu,[a] Linzi Qiu,[a] Yang Sheng,[a] Yixin Sun,[a] Linhong Deng,[b] Xinqing Li,[c] Mark Bradley[d] and Rong Zhang*[a]

Received 9th July 2017,
Accepted 15th December 2017

DOI: 10.1039/c7tb01851g

rsc.li/materials-b

Dual-drug loaded pH-responsive hydrogels were prepared as a delivery system carrying, as exemplars, both anti-cancer and anti-bacterial agents for pH controlled drug release. The hydrogels were composed of poly-(L-lactide)-*co*-polyethyleneglycol-*co*-poly(L-lactide) dimethacrylates (with various molecular weights of L-lactide oligomers) as a macromolecular crosslinker and copolymerized with acrylic acid and *N*-isopropylacrylamide. The biodegradability, biocompatibility and mechanical properties of the hydrogels were characterized with the hydrogels being nontoxic to cells, while showing a reversible >80% reduction in volume at pH 1.2 compared to pH 7.4. Drug release profiles showed differential release of tetracycline over doxorubicin at pH 1.2, with both drugs being released equally at pH 7.4. Biodegradability was tunable by altering the crosslinking density and pH, with the total degradation of the best gels observed within 2 weeks at pH 7.4.

## Introduction

Hydrogels are a class of materials that consist of a three-dimensional network of polymers which absorb large quantities of water. Biodegradable hydrogels are typically soft materials and have been used in multiple biomedical applications,[1–4] such as tissue engineering scaffolds and drug delivery carriers. They can include biodegradable components such as poly(lactic acid) (PLA),[5] poly(ε-caprolactone) (PCL),[6] poly(D,L-lactide-*co*-glycolide) (PLGA),[7] and poly(ε-caprolactone-*co*-lactide) (PCLA)[8] as hydrophobic blocks copolymerized with hydrophilic components such as poly(ethylene glycol) (PEG). Among the various classes of hydrogels developed, the copolymers of poly(L-lactide)-*co*-polyethyleneglycol-*co*-poly(L-lactide) (PLLA–PEG–PLLA) and their derivatives show promising potential in a number of biomedical applications, for example, with materials designed to form stable self-assembling micellar structures[9] with the hydrophobic core allowing good loading of hydrophobic drugs, while also undergoing biodegradation.[10,11] Moreover, the biodegradability of the synthesized PLLA–PEG–PLLA can be easily controlled by tuning the ratio of the lactide to PEG during the ring-opening polymerization process.[12,13] For example PDLA–PLLA–PEG–PLLA–PDLA pentablock copolymers have been synthesized and used for preparing micelles for the release of doxorubicin (DOX) in a controlled manner.[14] Other examples include drug encapsulation within nanogels[15,16] and liposomes,[17,18] with biocompatible hydrogels attracting considerable interest because of their low toxicity and biodegradability.[19–22]

Many hydrogels have been designed such that they respond to external factors such as light, magnetic fields, and enzymes or environmental factors such as pH and temperature. Examples include: (a) multi-responsive hydrogels of poly(methacrylic acid-*co*-*N*-vinylpyrrolidone) with a peptide crosslinker have been used as drug carriers for the oral delivery of insulin, with hydrogels retaining the insulin in simulated gastric fluid at pH 1.2, while releasing it at pH 6.8 due to the trypsin triggered cleavage of the peptide crosslinker.[23] (b) Photo-responsive hydrogels have been generated and used for controlled drug delivery.[24] This includes polymers that absorb light and undergo subsequent reversible thermally induced changes (and cargo release) to polymers that undergo irreversible bond cleavage and polymer dissolution.[25] (c) In the area of "magnetic hydrogels" numerous polymers have been designed[26] including magnetic hydrogel materials designed to be magnetically localized and those that are designed to undergo magnetically activated swelling, aggregation or degradation with the release of growth factors.[27] (d) The broad difference in pH between the stomach and other parts of the gastrointestinal (GI) tract allows pH-sensitive drug delivery systems to selectively deliver drugs. For example, the targeting of specific disease sites in the GI tract for local

[a] Jiangsu Key Laboratory of Environmentally Friendly Polymeric Materials, School of Materials Science and Engineering, Changzhou University, Changzhou 213164, China. E-mail: rzhang@cczu.edu.cn
[b] Institute of Biomedical Engineering and Health Sciences, Changzhou University, Changzhou 213164, Jiangsu, China
[c] Department of Plastic and Aesthetic Surgery, The Affiliated Second People's Hospital of Changzhou, Nanjing Medical University, Changzhou 213003, Jangsu, China
[d] School of Chemistry, EaStCHEM, University of Edinburgh, Joseph Black Building, West Mains Road, Edinburgh, EH93JJ, UK

† Electronic supplementary information (ESI) available: Additional methods and figures including FTIR spectra, GPC curves, gel content and yields of the hydrogels, LCST analysis, standard drug concentration curves, optical images of the hydrogels, HeLa cell viability, antibacterial images, a table of *E. coli* inhibition zones and their mechanical properties. See DOI: 10.1039/c7tb01851g

drug release or uptake/delivery of the drug *via*, for example, the small intestine. pH responsive polymers include: the block copolymer polyamidoamine–PLLA–PEG which forms micelles that show controlled drug release when the pH is low, while retaining the drug at pH 7.4;[28] poly(L-histidine)–PEG block copolymers which when mixed with PLLA–PEG generate micelles for controlled drug release, with the dissolution of the poly(L-histidine)–PEG and swelling of the micelles at pH 6.[29] Another pH sensitive material generated from the grafted copolymer of poly(*N*-isopropyl acrylamide-*co*-methacrylic acid)-*g*-PLA has also been used to prepare multifunctional micelles for cancer cell targeting and anticancer drug delivery.[30] (e) In addition smart drug carriers with dual environmentally responsive behaviours are being developed. Thus a pH and temperature sensitive hydrogel prepared from dextrin and poly(acrylic acid) has been used for sustained release of ornidazole and ciprofloxacin.[31] Some block copolymers show sol–gel transitions when the temperature is increased to 37 °C,[32,33] and these polymers have been used for dissolution of an anticancer drug with subsequent gelation upon injection.

In recent years, combination therapies have attracted much attention with the co-use of multiple drugs having both different therapeutic[34,35] and/or synergistic[33,36,37] effects. However the controlled dual administration of multiple drugs, each with their own distinct physical and chemical properties, is challenging. A hydrogel/micelle composite prepared from PEG and poly(vinyl alcohol) (PVA) with embedded tramadol, and oleic acid-*g*-chitosan copolymer micelles loaded with the antibiotic cefixime was developed as a dual-drug release carrier[38] allowing efficient release of two very different drugs. A drug carrier prepared from a CS/PVA hydrogel encapsulating aspirin and poly(L-glutamic acid)-*b*-poly(propylene oxide)-*b*-poly(L-glutamic acid) micelles entrapping DOX showed independent release behaviour of each drug.[39]

Dual drug release from hydrogels has been reported with the covalent attachment of polymeric micelles that possessed different drug release profiles.[34] pH sensitive protein–carbopol–polyacrylamide based hydrogels have been used to encapsulate a combination of antimalarial drugs (one highly water soluble and the other highly insoluble) with the hydrogel allowing controlled delivery/release of both drugs.[40]

Here hydrogels were designed to act as pH responsive "smart drug carriers" to allow controlled dual drug release, with materials fabricated using poly(L-lactide)-*co*-polyethyleneglycol-*co*-poly(L-lactide) dimethacrylates (MA–PLLA–PEG–PLLA–MA) as degradable polymeric crosslinkers along with the monomers acrylic acid (AA) and *N*-isopropylacrylamide (NIPAM). As model compounds the anticancer drug DOX and the antibiotic tetracycline (TET)[41,42] were loaded into the hydrogels with the dual drug loading efficiency and *in vitro* drug release at pH 7.4 and 1.2 examined. Experiments demonstrated that the dual-drug loaded hydrogels released drugs under differing conditions and successfully killed HeLa cells while inhibiting the growth of *Escherichia coli*.

# Experimental

### Materials

L-Lactide (LLA) was obtained from Sinobiom and recrystallized from dry ethyl acetate before use. PEG ($M_w$ 4000) and NIPAM were purchased from Aldrich. Stannous 2-ethyl-hexanoate ($Sn(Oct)_2$), methacrylic anhydride and Irgacure 2959 were purchased from Aike, and used as received. Dichloromethane and triethylamine (TEA) were dried over calcium hydride and distilled prior to use. Doxorubicin and tetracycline were purchased from MeilunBio.

### Synthesis of MA–(PLLA–PEG–PLLA)–MA

PEG (20 g, 5 mmol) and appropriate amounts of L-lactide (mole ratios used were 1 : 2 and 1 : 5) were mixed with the catalyst (3 wt‰ of total monomer weight) and heated for 12 h at 130 °C. The reaction mixture was cooled to room temperature and the solid was dissolved in dichloromethane (50 mL) before pouring the solution into excess diethyl ether. The precipitate was collected *via* centrifugation and the polymer diols were dried at 40 °C under vacuum for 24 hours. The PLLA–PEG–PLLA diols (20 g) were dissolved in 100 mL of dichloromethane, and triethylamine and methacrylic anhydride in dichloromethane (10 mL) were added dropwise (the molar ratio of PLLA–PEG–PLLA : TEA : MA was 1 : 4 : 4) and reacted at 30 °C for 48 hours to give the end-capped polymer diols (MA–PLLA–PEG–PLLA–MA) as reported by Lee.[11] The product was recovered *via* precipitation from a mixture of cold ether/hexane/methanol (10/1/1, v/v/v).

### Polymer characterization

The polymers were characterized using FTIR (Nicolet Avatar 370 spectrophotometer, Nicolet) and $^1$HNMR (AVANCEIII-400 spectrometer, 400 MHz) in $CDCl_3$ (see the ESI†). The molecular weights and polydispersity were measured using GPC (Waters Alliance 515) with THF as the eluent with a flow rate of 1 mL min$^{-1}$ on a Waters Styragel HR column calibrated using polystyrene standards.

### Preparation of hydrogels based on MA–PLLA–PEG–PLLA–MA

Hydrogels were prepared using MA–PLLA–PEG–PLLA–MA, AA and NIPAM in various ratios (Table 1). Thus MA–PLLA–PEG–PLLA–MA, AA and NIPAM were dissolved in deionized water (1.5 g) and 1 wt% of the photoinitiator I2959 (relative to the total mass of monomers). The solution was stirred under nitrogen for 30 min before being cast onto PTFE molds (12 mm in diameter, thickness 1 mm) and photo-polymerized under 365 nm UV light (SB-100P/FA) for 10 min. The hydrogels were soaked in 50 mL of distilled water for 48 hours to remove impurities or unreacted monomers before drying in a vacuum oven at 50 °C to a constant weight.

### Preparation of dual-drug loaded hydrogels

Each molded hydrogel "pellet" was submerged into phosphate-buffered saline (PBS, 8 mL, pH 7.4) containing DOX (50 μM) and TET (198 μM) in a 12-well plate for 48 hours. The hydrogel was removed to a new plate and the remaining drug was quantified (496 nm for doxorubicin and 361 nm for tetracycline) (for details please see the Methods section and Fig. S5 and S6 in the ESI†).

### Scanning electron microscopy (SEM)

SEM was used to visualize the morphology of the hydrogels. The hydrogels were immersed in deionized water at pH 1.2

Table 1 The hydrogels synthesized with various monomer/cross-linker combinations

| Polymers | (MA–PLLA–PEG–PLLA–MA)-2 or 5 : AA : NIPAM (wt%/molar ratio)[a] |
|---|---|
| S1 | 70:30 : 0/1 : 40 : 0 |
| S2 | 55 : 25 : 20/1 : 42 : 22 |
| S3 | 40 : 20 : 40/1 : 46 : 59 |
| S4 | 55 : 25 : 20/1 : 46 : 23 |
| S5 | 40 : 20 : 40/1 : 51 : 65 |

[a] Polymers S1–S3 used the macro cross-linker (MA–PLLA–PEG–PLLA–MA)-2 with PEG : LLA (1 : 2 (mol mol$^{-1}$)) and polymers S4 and S5 used the macro cross-linker (MA–PLLA–PEG–PLLA–MA)-5 with PEG : LLA (1 : 5 (mol mol$^{-1}$)).

(simulated gastric fluid) and pH 7.4 (simulated intestinal fluid) respectively for 48 hours and then frozen in liquid nitrogen before lyophilization for 48 hours. The cross-sections of the freeze-dried specimens were then sputtered with gold for 60 seconds before analysis *via* SEM (JSM-6510).

### Swelling analysis of hydrogels in buffers of various pHs

The swelling ratios of hydrogels were measured using a gravimetric method. The cylindrical hydrogel samples were immersed in PBS buffers at various pH values (pH 1.2, 4.0, 5.0, and 7.4) at 37 °C for 48 h. The samples were removed and excess fluid removed with filter paper before weighing (see the ESI†). The swelling behavior of the hydrogels was similarly studied at pH 1.2 after 0.5, 1, 2, 4, 8 and 12 h and at pH 7.4 after 0.5, 1, 2, 4, 8 and 12 h ($n$ = 3).

### *In vitro* biodegradation of the hydrogels

The degradation was studied by immersing the hydrogel pellets (50.9 ± 1.1 mg) in PBS (8 mL, 10 mM) at pH 7.4 or 1.2. The hydrogels were removed from the degradation solution at designed time points, washed with distilled water and dried to a constant weight in a 50 °C vacuum oven (see the ESI†).

### *In vitro* dual drug release

To measure the amount of released doxorubicin and tetracycline, the dual-drug loaded hydrogels were immersed at pH 1.2 or 7.4 at 37 °C with stirring (100 rpm). 4 mL of the solution from each vial was removed for analysis (absorbance at 496 nm and 361 nm) and replaced with an equal volume of the solution. The cumulative release of drugs was calculated (see the ESI†).

## Result and discussion

### Polymer synthesis and characterization

MA–PLLA–PEG–PLLA–MA was prepared and used as a macro cross-linker instead of the traditionally used small molecular cross-linkers such as *N*,*N*′-methylenebisacrylamide or glutaraldehyde to improve the hydrophobic properties and degradation abilities of the hydrogels to make them suitable for biological applications (Scheme 1 and Table 2). The synthesized polymers were characterized using $^1$H-NMR: the chemical shifts for resonance signals were assigned to the corresponding protons on PLLA–PEG–PLLA diols (Fig. 1a) including: 1.4 (m, CH(C$\underline{H}_3$)OH, end

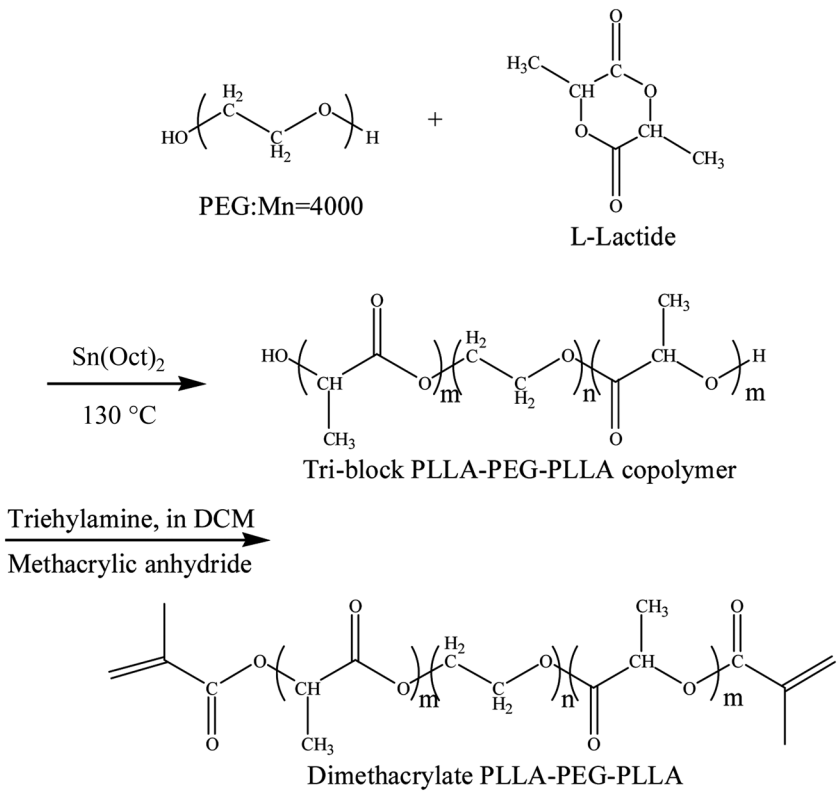


Scheme 1 Preparation of the macro crosslinker MA–PLLA–PEG–PLLA–MA.

 

group of PLLA), 1.5 (m, CHC$\underline{H}_3$ of PLLA), 3.6 (m, C$\underline{H}_2$–O–C$\underline{H}_2$ of PEG), 4.2–4.3 (m, C$\underline{H}_2$OCO, linking unit of PEG–PLLA), and 4.3–4.4 (q, C$\underline{H}$(CH$_3$)OH), 5.2 (m, C$\underline{H}$CH$_3$). The chemical shifts of protons on MA–PLLA–PEG–PLLA–MA included 1.4 (m, CH(C$\underline{H}_3$)OCO, end group of PLLA), 1.5 (m, CHC$\underline{H}_3$ of PLLA), 1.9 (s, C(C$\underline{H}_3$)═C$\underline{H}_2$), 3.6 (m, C$\underline{H}_2$–O–C$\underline{H}_2$ of PEG), 4.2–4.3 (m, C$\underline{H}_2$OCO, linking unit of PEG–PLLA), 4.3–4.4 (q, C$\underline{H}$(CH$_3$)OCO), 5.2 (m, C$\underline{H}$CH$_3$), and 5.6 and 6.2 ((CH$_3$)C═C$\underline{H}_2$) (Fig. 1b). FTIR analysis also indicated that the polymer diols and MA–PLLA–PEG–PLLA–MA were successfully prepared (see Fig. S1 in the ESI†). The molecular weight and chemical structure of polymer diols and their end-capped cross-linkers were calculated using $^1$HNMR. As shown in Fig. 1, the chemical shifts at 4.3–4.4 (C$\underline{H}$(CH$_3$)OCO–) correspond to the protons of the LLA units and those at 3.6 (–C$\underline{H}_2$–O–C$\underline{H}_2$–) correspond to the protons of the ethylene glycol units. Based on integration of the peak areas, the number of repeating units ($n$) of LLA and the molecular weight of the diols could be calculated (Table 2).[45] The molecular weights and polydispersity (PDI) of the synthesized polymers were also determined using GPC (Table 2), with the molecular weights of the PEG successfully increased by adjusting the molar ratio of LLA to PEG4000 from 2 : 1 to 5 : 1. The results indicate that the $M_n$ (NMR) values of the synthesized polymers were close to the theoretical molecular weight, while GPC analysis gave PDIs of about 1.1. Not surprisingly the GPC results of the polymer diols virtually overlapped with that of the functionalized MA–PLLA–PEG–PLLA–MA (see Fig. S2 in the ESI†).

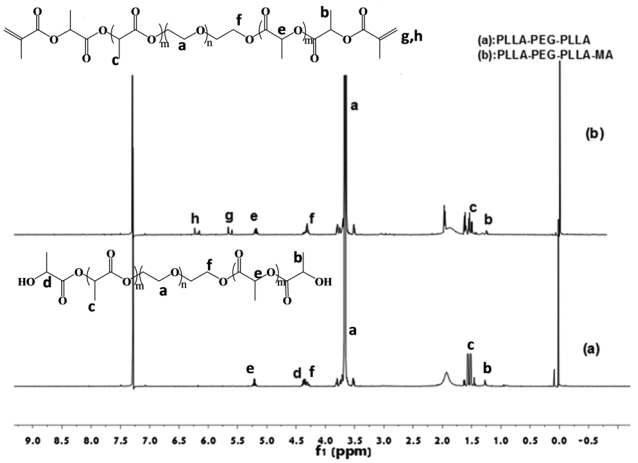


Fig. 1 $^1$H-NMR spectra of: (a) PLLA–PEG–PLLA copolymer diols and (b) the macro cross-linker MA–PLLA–PEG–PLLA–MA, both in CDCl$_3$.

## Swelling properties of the hydrogels

Hydrogels consisting of MA–PLLA–PEG–PLLA–MA, AA and NIPAM were prepared using a light mediated free radical polymerization approach in high yield (see Fig. S3 in the ESI†). The physical and chemical properties of the hydrogels could be tuned using MA–PLLA–PEG–PLLA–MA with different molecular weights of the PLLA segments. The swelling ratios of the hydrogels in aqueous media were shown to play important roles in their biodegradation behaviour. The variation of the swelling ratios for all hydrogels was small (less than one-fold increase) when increasing the pH from 1.2 to 5.0, although S4 was the most hydrophilic with about 500% swelling at pH 1.2. A critical change occurred when the pH was increased from 1.2 to 7.4 with the swelling ratios of the hydrogels increasing some 3.0 (S1), 2.9 (S2), 3.2 (S3), 3.6 (S4) and 8.4 (S5) fold. The rational for this increase in the swelling ratio with pH is presumably due to ionization and subsequent repulsion between the poly(acrylic acid) units at pH 7.4, which makes the hydrogels hydrophilic. These results indicate that the molecular weight of MA–PLLA–PEG–PLLA–MA influences the pH response of the hydrogels, with MA–PLLA–PEG–PLLA–MA with the highest molecular weight showed the largest swelling ratio as the pH increased to 7.4 (Fig. 2A).

Table 2 Molecular weight and polydispersity index of the synthesized PLLA–PEG–PLLA diols and MA–PLLA–PEG–PLLA–MAs

| | | Molecular weight | | | |
|---|---|---|---|---|---|
| | | | | GPC | |
| Polymer | Yield (%) | Theory | $^1$H-NMR | $M_n$ | PDI |
| PLLA–PEG–PLLA-2 | 91 | 4288 | 4136 | 6400 | 1.12 |
| MA–PLLA–PEG–PLLA–MA-2 | 85 | 4442 | 4410 | 6700 | 1.11 |
| PLLA–PEG–PLLA-5 | 93 | 4720 | 4484 | 7000 | 1.14 |
| MA–PLLA–PEG–PLLA–MA-5 | 82 | 4874 | 4808 | 7300 | 1.13 |

Note: the theoretical molecular weight was calculated from the monomer inputs. The actual molecular weight was calculated *via* $^1$H-NMR following our reported method.[43]

The reversible swelling (pH 7.4) and de-swelling (pH 1.2) of the hydrogels could be repeated over many cycles (Fig. 2B) with the hydrogels shrinking dramatically over 2 hours with some of them (*i.e.* S3, S5) becoming opaque (Fig. 2C) showing the formation of a hydrophobic phase in the gels. The transmittance of the hydrogels changed as the temperatures increased above 25 °C, showing the existence of a lower critical solution temperature (LCST) (see Fig. S4 in the ESI†). The LCST of the hydrogels showed an abrupt change when the hydrogels had more NIPAM and less MA–PLLA–PEG–PLLA–MA, such as hydrogels S3 (31 °C) and S5 (29 °C) which were hydrophobic with low swelling ratios in acidic buffers at 37 °C. The LCST of S4 was 36 °C and the polymer was transparent at room temperature. The average pore size, measured from SEM images of the frozen dried hydrogels (Fig. 2D and E) showed at pH 7.4 was *ca.* 8 μm in diameter, which reduced to *ca.* 2 μm or less at pH 1.2.

## *In vitro* degradation of the hydrogels

As shown in Fig. 3A and B, hydrogels S4 and S5 degrade more quickly than the other three samples presumably because the low cross-linking density allows greater buffer accessibility and resulted in faster swelling and degradation.

At pH 7.4 the degradation rate increased with the reduction of the macro cross-linker loading (S1 < S2 < S3 (70%/55%/40%)), while at pH 1.2 the degradation rate was inverted (S1 > S2 > S3) (Fig. 3C). Ester hydrolysis can be either acid or base mediated, while solvent accessibility and polymer mobility are also important features as is internal catalysis in

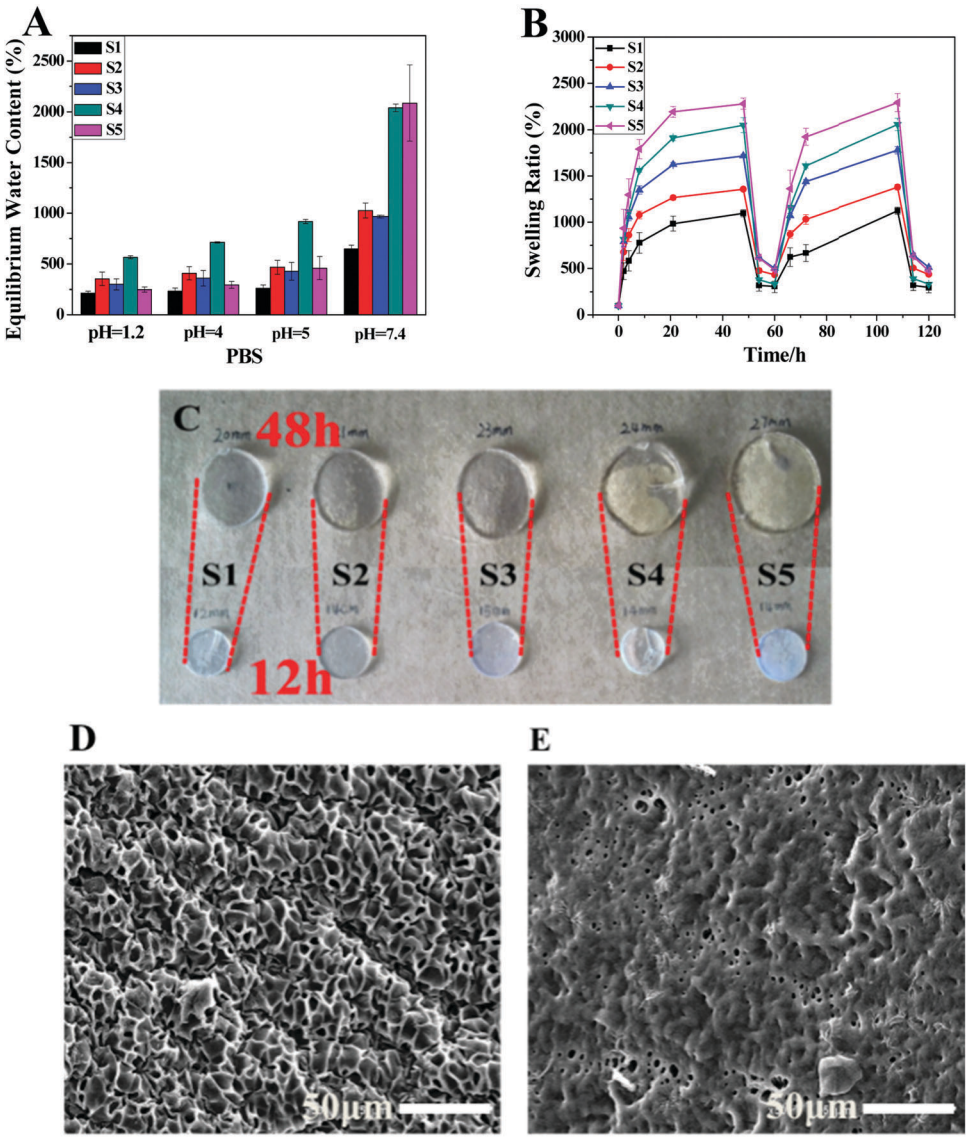


Fig. 2 Properties of the hydrogels. (A) Equilibrium water content of hydrogels at various pH values at 37 °C, $n$ = 3; (B) swelling of the hydrogels with switching between pH 7.4 (high swelling ratios) and 1.2 (low swelling ratios) at 37 °C; (C) images of the hydrogels at pH 7.4 (upper) and 1.2 (lower) at equilibrium; (D) SEM images of hydrogels swollen at pH 7.4 and (E) pH 1.2 and then frozen and lyophilized. The average pore size of hydrogels was calculated using Image J.

the form of carboxylic acid groups. Not unexpectedly it was found that the buffer became acidic after two weeks of hydrogel degradation due to ester hydrolysis (Fig. 3D) – an observation commonly found around PLA based implants.

### Drug release from the hydrogels

Analysis of the drug loading of the hydrogels (Fig. 4 and Fig. S5, S6 in the ESI†) showed that the hydrogels typically loaded more DOX than TET. This was probably through hydrophobic interactions and aggregation with the PLLA segments in the hydrogels because DOX ($\log p$ 2.82) is more hydrophobic than TET ($\log p$ −1.47). S4 and S5 with the longer crosslinkers loaded more TET than other hydrogel samples. As for DOX, the ratio of the macro crosslinker and NIPAM was an important factor that influenced drug loading, with S2 loading similar amounts of DOX as S5.

Drug release experiments showed that DOX was released less at pH 1.2 than that at pH 7.4 (Fig. 5 and Fig. S7 in the ESI†) with the accumulative release of only 20–23% after 10 hours in PBS at pH 1.2 for hydrogels S1 and S2, while it increased to 52% at pH 7.4 after 10 hours (Fig. 5A and B). The drug release from S3, S4 and S5 was 43%, 42% and 47%, respectively, under acidic conditions; however, this was increased to 62% for S3 and S5 and 52% for S4 at pH 7.4. The reason why hydrogels S3, S4 and S5 released more than S1 and S2 at pH 1.2 is probably due to several reasons: firstly the levels of the macro crosslinker in S3 or S5 were less than those in S1 or S2, with more DOX released from the "looser" hydrogels at pH 1.2;[44] secondly, although the macro crosslinker of S4 was similar to that of S2, the swelling

 

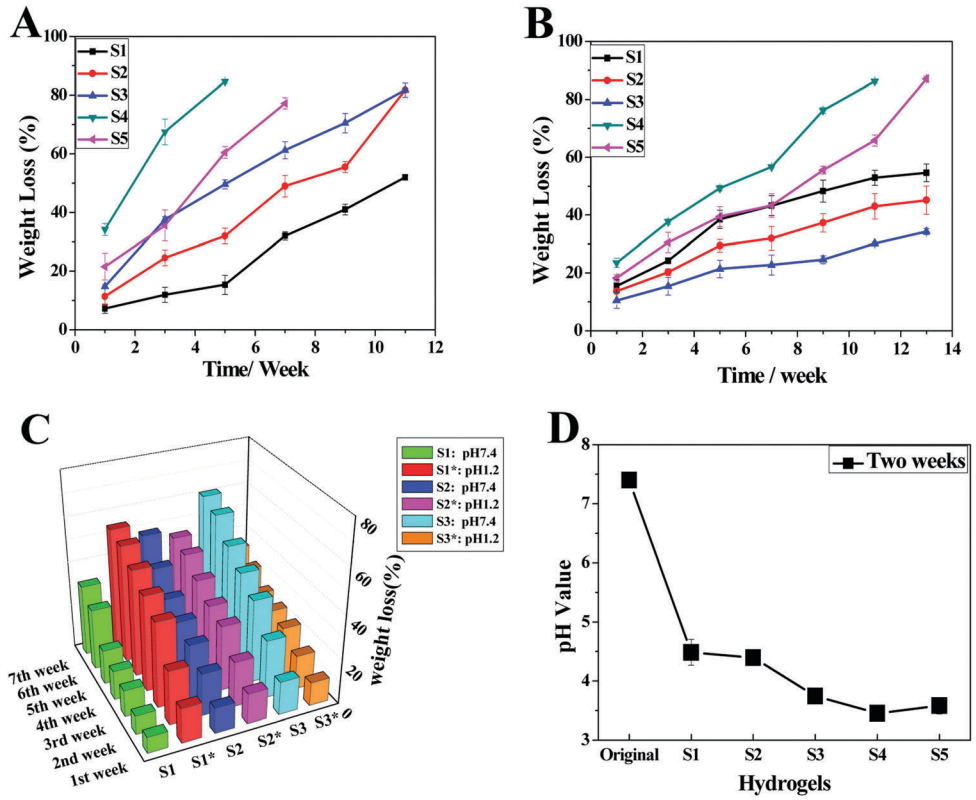


Fig. 3 Biodegradation analysis of hydrogels. (A) The biodegradable behavior of the hydrogels at pH 7.4 with S4 and S5 showing total degradation after 6 and 8 weeks, respectively; (B) the biodegradable behavior of the hydrogels at pH 1.2; (C) the difference in the biodegradation rate of the hydrogels (S1–3) in various environments; and (D) the pH value change of the degradation buffers when the hydrogels degraded in PBS (beginning at pH 7.4) after 2 weeks.

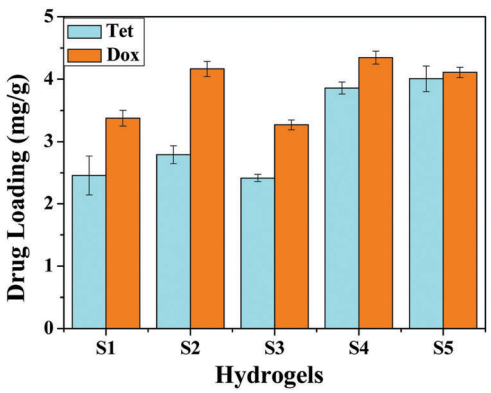


Fig. 4 Dual-drug loading of hydrogels. The dual-drug solutions used for the drug loading were 50 μM DOX and 200 μM TET in PBS (pH 7.4). The errors are STDEV and $n$ = 3.

ratio at pH 1.2 was larger than S2 or S1 (Fig. 2A), thus more DOX was released from S4. However, the TET release profiles of hydrogels told a very different story (Fig. 5C and D). In acidic buffer, the accumulative release increased from 65% for S1 to 95% for S5, with the drug release from S4 and S5 reaching >95% in just 2 hours. The TET release at pH 7.4 ranged from 60 to 78% for S1–S5.

The drug loaded hydrogels S1–S5 released 31–61% of the doxorubicin cargo into the supernatant after 12 hours (see Fig. S9 in the ESI†). This doxorubicin, liberated from the hydrogel carriers, was effective in killing HeLa cells and showed analogous levels of cell death to the equivalent level of free DOX (Fig. S9C in the ESI†). The cytotoxicity of the hydrogels themselves was evaluated in a CCK-8 assay with the degraded polymers showing low toxicity to cells (see Fig. S8 in the ESI†), in agreement with the results of the other hydrogels.[45,46]

Antibacterial experiments showed that the dual-drug loaded hydrogels formed inhibition zones on agar surfaces coated with *E. coli* after 24 h of incubation (see the Methods section, Fig. S10 in the ESI†). S4 and S5 were more effective in bacterial killing than the other three hydrogel samples (while no inhibition zone was formed around the controls), agreeing with the above results that S4 and S5 loaded more TET than the other hydrogels (Fig. 4).

The mechanical properties of the hydrogels were analyzed *via* compressive tests and rheological measurements (see Fig. S11 in the ESI†) and showed that the hydrogels were stable, cross-linked hydrogels with compressive moduli ranging from 110 KPa (S1) to 4 KPa for S5.

## Conclusions

In summary, degradable copolymers MA–PLLA–PEG–PLLA–MA were synthesized and characterized and used as macro cross-linkers in the generation of hydrogels for the entrapment of two model drugs. The dual-drug loaded hydrogels based on MA–PLLA–PEG–PLLA–MA, AA and NIPAM showed that biodegradability

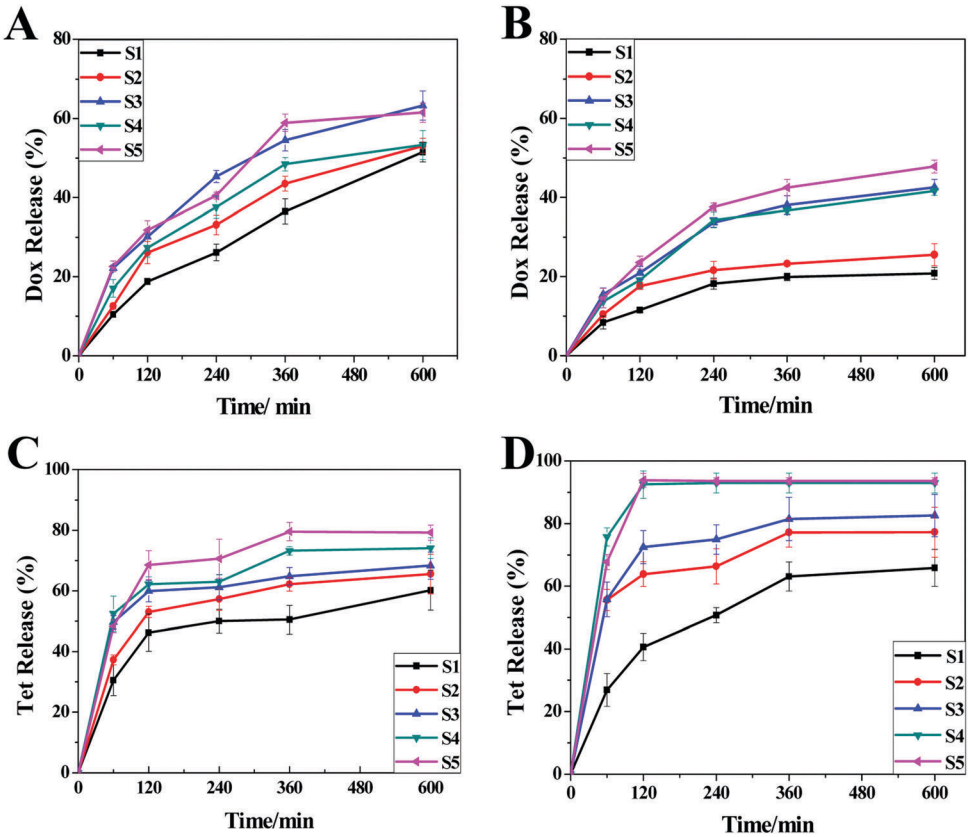


Fig. 5 Drug release profiles of TET and DOX from hydrogels S1–S5 at 37 °C. (A and C): pH 7.4 and (B and D): pH 1.2. The errors were STDEV and $n$ = 3.

of the hydrogels could be controlled using specific macromolecular cross-linkers with appropriate molecular weights. Analysis showed that the hydrogels were pH sensitive, with all the hydrogels shrinking at pH 1.2 and swelling at pH 7.4. At pH 7.4 the hydrophobicity was an important factor that controlled degradation rate, with hydrogels with higher levels of hydrophobic segments (like S1) degrading more slowly than the less hydrophobic S3. On the other hand, at pH 1.2 all of the hydrogels became more hydrophobic and [$H^+$] became an important factor in controlling the degradation rate of the hydrogels – presumably by catalyzing and accelerating the hydrolysis of the polyester cross-linker. Higher percentages of the macro cross-linker in hydrogels such as in S1 lead to more rapid degradation. The influences of pH and monomer combination on the swelling ratio and drug-releasing rate of the hydrogels were examined using simulated gastric fluid (pH 1.2) and simulated intestinal fluid (pH 7.4). The release of DOX was considerably slower at pH 1.2 than that at pH 7.4 due to the hydrophobic hydrogel preventing the drug from quickly dissolving/being liberated from the scaffold, while the liberated DOX was effective in killing HeLa cells. TET was "burst released" from the hydrogels at pH 1.2 due to the hydrophilicity of the drug. An antibacterial study showed that the hydrogels loaded with TET liberated the antibacterial agent and killed *E. coli* in a disk diffusion assay. The hydrogels' pH mediated differential drug release functionality (slow release of DOX in acidic buffers and the rapid release of TET) shows that the hydrogels have interesting drug carrier properties. TET showed a "burst release" behaviour at pH 1.2 (analogous to the stomach region) especially for hydrogels S4 and S5 over the first 1–2 hours, whilst most of the DOX was retained in the hydrogels at pH 1.2 and it was released at pH 7.4 (the pH found in the intestine or colon). This differential release profile of two drugs could thus be of benefit for the delivery of specific individual drugs to specific GI sites following, for example, oral administration.

## Conflicts of interest

There are no conflicts of interest to declare.

## Acknowledgements

We gratefully acknowledge the support from the National Natural Science Foundation of China (21374012, 11532003, and 51563003), Jiangsu Province for support under the distinguished professorship program, and the Priority Academic Program Development (PAPD) of Jiangsu Higher Education Institutions. We would also like to thank the Start-up funding (ZMF15020107) from Changzhou University and the Natural Science Foundation of Jiangsu Province (BK20160278) for supporting DrYang Sheng, Natural Science Foundation of Guangxi Province (2015GXNSFAA139255) for supporting DrYixin Sun, and MBR thanks the ERC (ERC-2013-ADG 340469 ADREEM).

 

## Notes and references


1 D. E. Fullenkamp, J. G. Rivera, Y. K. Gong, K. H. A. Lau, L. H. He, R. Varshney and P. B. Messersmith, *Biomaterials*, 2012, **33**, 3783–3791.
2 H. N. Lim, N. M. Huang, S. S. Lim, I. Harrison and C. H. Chia, *Int. J. Nanomed.*, 2011, **6**, 1817–1823.
3 Y. L. Li, J. Rodrigues and H. Tomas, *Chem. Soc. Rev.*, 2012, **41**, 2193–2221.
4 X. H. Hu, H. P. Tan and L. Y. Hao, *J. Mech. Behav. Biomed. Mater.*, 2016, **64**, 43–52.
5 J. G. Sun, X. Liu, Y. Lei, M. Y. Tang, Z. X. Dai, X. W. Yang, X. B. Yu, L. Yu, X. H. Sun and J. D. Ding, *J. Mater. Chem. B*, 2017, **5**(31), 6400–6411.
6 X. Liu, X. H. Chen, M. X. Chua, Z. B. Li, X. J. Loh and Y. L. Wu, *Adv. Healthcare Mater.*, 2017, **6**(11), 1700159.
7 M. McKenzie, D. Betts, A. Suh, K. Bui, R. Tang, K. X. Liang, S. Achilefu, G. S. Kwon and H. Cho, *Pharm. Res.*, 2016, **33**(9), 2298–2306.
8 H. J. Sim, T. Thambi and D. S. Lee, *J. Mater. Chem. B*, 2015, **3**(45), 8892–8901.
9 D. G. Abebe, K. Y. Liu, S. R. Mishra, A. H. F. Wu, R. N. Lamb and T. Fujiwara, *RSC Adv.*, 2015, **5**(116), 96019–96027.
10 K. Nagahama, J. Ohmura, H. Sakaue, T. Ouchi, Y. Ohya and N. Yui, *Chem. Lett.*, 2010, **39**, 250–251.
11 W. C. Lee, Y. C. Li and I. Chu, *Macromol. Biosci.*, 2006, **6**, 846–854.
12 R. C. Mundargi, V. R. Babu, V. Rangaswamy, P. Patel and T. M. Aminabhavi, *J. Controlled Release*, 2008, **125**, 193–209.
13 L. Yu, Z. Zhang and J. D. Ding, *Biomacromolecules*, 2011, **12**, 1290–1297.
14 H. L. Mao, G. R. Shan, Y. Z. Bao, Z. L. Wu and P. J. Pan, *Soft Matter*, 2016, **12**, 4628–4637.
15 H. Asadi, K. Rostamizadeh, D. Salari and M. Hamidi, *Int. J. Pharm.*, 2011, **416**, 356–364.
16 P. R. Sarika, P. R. Anil Kumar, K. R. Deepa and D. K. Raj, *Mater. Sci. Eng., C*, 2016, **68**, 251–257.
17 T. M. Allen and P. R. Cullis, *Adv. Drug Delivery Rev.*, 2013, **65**, 36–48.
18 C. Yao, P. Y. Wang, X. M. Li, X. Y. Hu, J. L. Hou, L. Y. Wang and F. Zhang, *Adv. Mater.*, 2016, **28**, 9341–9348.
19 P. Ferruti, S. Bianchi, E. Ranucci, F. Chiellini and A. M. Piras, *Biomacromolecules*, 2005, **6**, 2229–2235.
20 T. Zırıh and N. Orakdogen, *Eur. Polym. J.*, 2016, **75**, 371–387.
21 Y. Liang and K. L. Kiick, *Biomacromolecules*, 2016, **17**, 601–614.
22 C. B. Yang, D. X. Li, Q. Q. FengZhao, L. Y. Wang, L. Wang and Z. M. Yang, *Org. Biomol. Chem.*, 2013, **11**, 6946–6951.
23 J. M. Knipe, F. Chen and N. A. Peppas, *Biomacromolecules*, 2015, **16**, 962–972.
24 Y. Zhao, *Macromolecules*, 2012, **45**, 3647–3657.
25 Z. Zhou, Q. Yi, T. Xia, W. Yin, A. A. Kadi, J. Li and Y. Zhang, *Org. Biomol. Chem.*, 2017, **15**, 2191–2198.
26 Y. Li, G. Huang, X. Zhang, B. Li, Y. Chen, T. Lu, T.-J. Lu and F. Xu, *Adv. Funct. Mater.*, 2013, **23**, 660–672.
27 E. D. Silva, P. S. Babo, R. Costa-Almeida, R. M. A. Domingues, B. B. Mendes, E. Paz, P. Freitas, M. T. Rodrigues, P. L. Granja and M. E. Gomes, *Nanomedicine*, 2017, DOI: 10.1016/j.nano.2017.06.002.
28 J. T. Guo, H. Hong, G. J. Chen, S. X. Shi, Q. F. Zheng, Y. Zhang, C. P. Theuer, T. E. Barnhart, W. B. Cai and S. Q. Gong, *Biomaterials*, 2013, **34**, 8323–8332.
29 H. Q. Yin, E. S. Lee, D. I. Kim, K. H. Lee, K. T. Oh and Y. H. Bae, *J. Controlled Release*, 2008, **126**, 130–138.
30 C. K. Huang, C. L. Lo, H. H. Chen and G. H. Hsiue, *Adv. Funct. Mater.*, 2007, **17**, 2291–2297.
31 D. Das, P. Ghosh, S. Dhara, A. B. Panda and S. Pal, *ACS Appl. Mater. Interfaces*, 2015, **7**, 4791–4803.
32 M. Miyazaki, T. Maeda, K. Hirashima, N. Kurokawa, K. Nagahama and A. Hotta, *Polymer*, 2017, **115**, 246–254.
33 X. L. Li, R. R. Fan, Y. L. Wang, M. Wu, A. P. Tong, J. Shi, M. L. Xiang, L. X. Zhou and G. Guo, *RSC Adv.*, 2015, **5**, 101494–101506.
34 M. Murata, Y. Uchida, T. Takami, T. Ito, R. Anzai, S. Sonotaki and Y. Murakami, *Colloids Surf., B*, 2017, **153**, 19–26.
35 C. Y. Gong, C. Wang, Y. J. Wang, Q. J. Wu, D. D. Zhang, F. Luo and Z. Y. Qian, *Nanoscale*, 2012, **4**, 3095–3104.
36 X. L. Wu, C. L. He, Y. D. Wu and X. S. Chen, *Biomaterials*, 2016, **75**, 148–162.
37 K. A. Gilmore, M. W. Lampley, C. Boyer and E. Harth, *Adv. Drug Delivery Rev.*, 2016, **98**, 77–85.
38 T. S. Anirudhan, J. Parvathy and A. S. Nair, *Carbohydr. Polym.*, 2016, **136**, 1118–1127.
39 L. Wei, C. H. Cai, J. P. Lin and T. Chen, *Biomaterials*, 2009, **30**, 2606–2613.
40 B. A. Aderibigbe and Z. Mhlwatika, *J. Appl. Polym. Sci.*, 2016, **133**, 43918.
41 J. M. Wang, P. Yang, M. M. Cao, N. Kong, W. R. Yang, S. Sun, Y. Meng and J. Q. Liu, *Talanta*, 2016, **147**, 184–192.
42 L. H. Weng, N. Rostambeigi, N. D. Zantek, P. Rostamzadeh, M. Bravo, J. Carey and J. Golzarian, *Acta Biomater.*, 2013, **9**, 8182–8191.
43 X. P. Feng, G. R. Wang, K. Neumann, W. Yao, L. Ding, S. Y. Li, Y. Sheng, Y. Jiang, M. Bradley and R. Zhang, *Mater. Sci. Eng., C*, 2017, **74**, 270–278.
44 W. J. Zhang, P. F. Jiang, J. Chen, C. N. Zhu, Z. W. Mao and C. Y. Gao, *J. Colloid Interface Sci.*, 2017, **490**, 181–189.
45 P. L. Lai, D. W. Hong, K. L. Ku, Z. T. Lai and I. M. Chu, *Nanomedicine*, 2014, **10**(3), 553–560.
46 B. Jiang, B. Akar, T. M. Waller, J. C. Larson, A. A. Appel and E. M. Brey, *Acta Biomater.*, 2014, **10**, 1177–1186.